Lithium-Ion Battery Pack State of Charge and State of Energy Estimation Algorithms Using a Hardware-in-the-Loop Validation

Yongzhi Zhang, Rui Xiong, *Senior Member, IEEE*, Hongwen He, *Senior Member, IEEE*, and Weixiang Shen, *Member, IEEE*

***Abstract*—An adaptive H infinity filter approach is proposed to estimate the multistates including state of charge (SOC) and state of energy (SOE) for a lithium-ion battery pack. In the proposed approach, the covariance matching technique is used to adaptively update the covariance of system and observation noises and the recursive least square method is used to identify the battery model parameters in real time. The hardware-in-the-loop (HIL) platform for battery charge/discharge is set up to evaluate the accuracy and robustness of the SOC and the SOE estimation and compare the proposed approach with the multistate estimators using an extended Kalman filter and an H infinity filter. The experimental results indicate that the adaptive H infinity filter-based estimator is able to estimate the battery states in real time with the highest accuracy among the three filters.**

***Index Terms*—Adaptive H infinity filter, hardware-in-the-loop (HIL), lithium-ion batteries, multistate estimation.**

I. Introduction

LITHIUM-ION (Li-ion) batteries have found wide application in electric vehicles (EVs) due to their high energy density, high power density, low self-discharge, and long life. To provide sufficient power and energy for EVs, a battery pack that consists of hundreds or thousands of batteries connected in series and parallels is required. The state of charge (SOC) and state of energy (SOE) are two important quantities to indicate the status of the battery pack. The SOC indicates the battery remaining capacity and the SOE is a gauge of the battery remaining energy. Their accurate estimation can help manage battery pack efficiently, extend battery pack life, and extend EV driving range [1]–[3].

Five mathematical models based on state-space equations to capture the dynamics of Li-ion batteries in hybrid electric vehicles (HEVs) are proposed in [4]. A study of 12 lumped battery models is also conducted in [5]. The simulation results [4], [5] show that the models with a single state provide reasonable accuracy with simplicity, while the models including hysteresis and more states improve the model accuracy but at the cost of complexity, namely heavy computation burden [6]. Thus, the selection of the battery model is the balance between accuracy and complexity. In real applications, a simple battery model is preferred due to low computation burden, robustness, and reasonable accuracy. The combined model is one of such simple models used in the SOC estimation [7] and the SOC and SOE estimation [8]. In these two cases, robust performance and accurate estimation results are achieved. Therefore, the combined model will be selected in this study.

Currently, the Kalman filter (KF) is one of the most popular methods to estimate battery state in EVs [9]–[12]. For the KF, it is assumed that the dynamic model of the battery and the statistical properties of the exogenous inputs of the batteries are known. In practice, the constructed battery model and assumed knowledge about noise statistics based on experience usually have a certain error, which will easily cause filter instability or divergence. The improved KFs have been proposed to design the robust estimators for battery states in handling modeling errors and noise uncertainty [7], [13]–[15]. For example, the AEKF is introduced to estimate the SOC of a lead-acid battery in [7]. The results show that the AKEF provides smaller SOC estimation error than the EKF because of its adaptive ability to update the process and measurement noise covariance values. The sigma-point Kalman filter (SPKF) is proposed to estimate the SOC in [13] and the results show that the SPKF gives better estimation results in strong nonlinear battery systems than the EKF with lower root-mean-square error and lower maximum error. However, these approaches cannot solve the existing defects of KFs fundamentally since all these KF-based approaches require the assumption that the battery model is accurately established.

In contrast to the KF, the H infinity filter allows uncertainty in battery dynamic model and its filter accuracy does not depend on the specific noise statistics. Hence, it is more robust to disturbances in battery dynamics model and noise statistics

Manuscript received March 16, 2016; revised June 27, 2016; accepted August 17, 2016. Date of publication August 26, 2016; date of current version February 11, 2017. This work was supported by the National Natural Science Foundation of China under Grant 51507012. Recommended for publication by Associate Editor Y.-M. Chen. *(Corresponding authors: Rui Xiong and Hongwen He.)*

Y. Zhang is with the National Engineering Laboratory for Electric Vehicles, School of Mechanical Engineering, Beijing Institute of Technology, Beijing 100081, China (e-mail: zhangyz0130@163.com).

R. Xiong and H. He are with the National Engineering Laboratory for Electric Vehicles, School of Mechanical Engineering, Beijing Institute of Technology, Beijing 100081, China and also with Collaborative Innovation Center of Electric Vehicles in Beijing, Beijing Institute of Technology, Beijing 100081, China (e-mail: rxiong@bit.edu.cn; hwhebit@bit.edu.cn).

W. Shen is with the Faculty of Science, Engineering and Technology, Swinburne University of Technology, Hawthorn, Vic. 3122, Australia (e-mail: wshen@swin.edu.au).

Color versions of one or more of the figures in this paper are available online at http://ieeexplore.ieee.org.

Digital Object Identifier 10.1109/TPEL.2016.2603229

[16]–[22]. In [16], an H infinity filter approach is presented for robust parameter estimation in electrical capacitance tomography. It demonstrates better performance of the H infinity filter than other methods (in particular KFs) in handling model errors. The H infinity filter is also applied to the battery area which realizes the accurate parameter and state estimation, respectively, [17], [18]. In addition, the H infinity filter has been applied to mechanical vibration, networked control system, sampled-data system, and landing gear [19]–[22]. They all obtain the satisfactory state estimation results. When the H infinity filter applies to nonlinear systems, the extended H infinity filter is developed [23]–[25] by linearizing nonlinear systems. For the extended H infinity filter to circumvent the linearization error, the unscented transform is applied, leading to the unscented H infinity filter [26], which is similar to the unscented KF (UKF). The unscented H infinity filter is used to estimate power quality disturbances and prove that its performance is better than that of the UKF [27]. Although an H infinity filter generally is more robust than KFs [18], it is still assumed that the covariance values of the process and measurement noises are known. However, these covariance values may not be known exactly in real applications. Furthermore, the erroneous covariance can lead to large estimation error or divergence of the H infinity filter. Thus, the covariance values can be treated as design parameters in the adaptive H infinity filter [7] and can be estimated in real time to improve the performance of the H infinity filter. The adaptive H infinity filter is proposed in [28] to estimate the battery SOC and the experimental results indicate that its performance is better than that of the adaptive extended KF and the square root UKF. However, the adaptive H infinity filter for the SOC estimation in [28] lacks the details in deriving the adaptive algorithms for estimating covariance matrices and it is only evaluated offline, which ignores measurement noises, random disturbances, and real-time computing ability in real applications.

Besides the KF and H infinity filter methods, there are many other techniques to estimate the SOC. The recursive least square (RLS) algorithm is augmented to the observer for online SOC estimation based on the commonly used single particle model in [29]. The simulation results have shown good performance and effectiveness of the RLS algorithm based observer for battery state estimation. An estimator based on particle filter is proposed for the joint estimation of SOC and SOE in [8]. The experimental results have verified the accuracy and robustness of the SOC and SOE estimation under dynamic temperature conditions. A dual neural network (NN) fusion model which is composed of the linear NN battery model and back of prorogation NN is proposed to capture the behavior of open-circuit voltage and SOC in [30] and the accuracy and effectiveness of the NN model is also verified by the experimental results.

A. Contribution of the Paper

Both the SOC and the SOE are two important parameters for battery management system in EVs. Their accurate estimations have recently been the research focuses [4], [6], [31]–[34], particularly the SOE estimation. From engineering point of view, the SOE is more useful since it takes battery terminal voltage into account which can predict the available energy for EVs. In this paper, an adaptive H infinity filter based battery multistate estimators are constructed to estimate the battery SOC and SOE and an RLS approach is applied to identify the battery model parameters in real time. The adaptive H infinity filter is able to adjust its process and measurement noise matrices based on the covariance matching technique to further improve robustness compared to the H infinity filter. A hardware-in-the-loop (HIL) test bench for battery charge/discharge is set up to evaluate the adaptive H infinity filter based estimators for the SOC and the SOE in terms of their accuracy, computing ability, and robustness against disturbances and erroneous initial system parameters.

B. Organization of the Paper

In Section II, the adaptive H infinity filter approach is modeled; and Section III presents the battery modeling process for parameter identification and battery multistate estimation; Section IV introduces the experimental design and test bench; the experimental results are analyzed in Section V, followed by the conclusions in Section VI.

II. Adaptive H Infinity Filter Approach

In this section, a brief introduction of the H infinity filter approach and the detailed derivation process for an adaptive H infinity filter is presented.

A. Introduction of the H Infinity Filter Method

Suppose there is the linear discrete-time state-space equation expressed as

$$\begin{cases} x_k = F_{k-1}x_{k-1} + w_k \\ y_k = H_k x_k + v_k \\ \varepsilon_k = L_k x_k \end{cases} \tag{1}$$

where w_k and v_k are random noises with possibly unknown statistics or deterministic, ε_k is a linear combination of the state, and L_k is a matrix defined by the user. The goal is to estimate ε_k and if x_k is directly estimated, then there is a need to set $L_k = I$. $\hat{\varepsilon}_k$ and $\hat{x}_0$, respectively, represent the estimate of ε_k and the state at the initial time. Applying the game theory to the H infinity filter method results in the following cost function [35]:

$$J_1 = \frac{\sum_{k=0}^{N-1} \|\varepsilon_k - \hat{\varepsilon}_k\|_{S_k}^2}{\|x_0 - \hat{x}_0\|_{P_0^{-1}}^2 + \sum_{k=0}^{N-1} \left(\|w_k\|_{Q_k^{-1}}^2 + \|v_k\|_{R_k^{-1}}^2 \right)} \tag{2}$$

where S_k, P_0, Q_k, and R_k are symmetric matrices selected by the user according to the particular problem.

Since J_1 is not easily to be directly minimized, as a replacement, a performance bound is chosen to explore an optimal estimation strategy making sure that J_1 satisfies the threshold, namely finding an estimate of ε_k, which leads to

$$J_1 < \frac{1}{\tau} \tag{3}$$

where τ is the user-specified performance bound. The calculation process of the discrete-time H infinity filter is shown in Table I.

TABLE I
H INFINITY FILTER CALCULATION PROCESS

$$\textbf{System equations:}\begin{cases} x_k = F_{k-1}x_{k-1} + w_k \\ y_k = H_k x_k + v_k \\ \varepsilon_k = L_k x_k \end{cases} \quad (4)$$

I Initialization: for $k = 0$, set

$$\hat{x}_0^+ = E(x_0), P_0^+ = E\left[\left(x_0 - \hat{x}_0^+\right)\left(x_0 - \hat{x}_0^+\right)^T\right], S_0, \theta, Q_0, R_0 \quad (5)$$

II Time update: For $k = 1, 2, \ldots$, compute

Prior estimate of state: $\hat{x}_k^- = F_{k-1}\hat{x}_{k-1}^+$ (6)

Prior estimate of error covariance: $P_k^- = F_{k-1}P_{k-1}^+F_{k-1}^T + Q_{k-1}$ (7)

Symmetric positive definite matrices update: $\bar{S}_k = L_k^T S_k L_k$ (8)

Condition judgment: $(P_k^-)^{-1} - \theta\bar{S}_k + H_k^T R_k^{-1} H_k > 0$ (9)

III Measurement update:

Innovation update: $e_k = y_k - H_k\hat{x}_k^-$ (10)

Kalman gain matrix update: (11)

$K_k = F_k P_k^-(I - \theta\bar{S}_k P_k^- + H_k^T R_k^{-1} H_k P_k^-)^{-1} H_k^T R_k^{-1}$

Measurement update of state estimate: $\hat{x}_k^+ = \hat{x}_k^- + K_k e_k$ (12)

Measurement update of error covariance: (13)

$P_k^+ = P_k^-(I - \theta\bar{S}_k P_k^- + H_k^T R_k^{-1} H_k P_k^-)^{-1}$

TABLE II
ADAPTIVE H INFINITY FILTER CALCULATION PROCESS

$$\textbf{System equations:}\begin{cases} x_k = F_{k-1}x_{k-1} + w_k \\ y_k = H_k x_k + v_k \\ \varepsilon_k = L_k x_k \end{cases} \quad (23)$$

I Initialization: for $k = 0$, set

$$\hat{x}_0^+ = E(x_0), P_0^+ = E\left[(x_0 - \hat{x}_0^+)(x_0 - \hat{x}_0^+)^T\right], S_0, \theta, Q_0, R_0 \quad (24)$$

II Time update: For $k = 1, 2, \ldots$, compute

Prior estimate of state: $\hat{x}_k^- = F_{k-1}\hat{x}_{k-1}^+$ (25)

Prior estimate of error covariance: $P_k^- = F_{k-1}P_{k-1}^+F_{k-1}^T + Q_{k-1}$ (26)

Symmetric positive definite matrices update: $\bar{S}_k = L_k^T S_k L_k$ (27)

Condition judgment: $(P_k^-)^{-1} - \theta\bar{S}_k + H_k^T R_k^{-1} H_k > 0$ (28)

III Measurement update:

Innovation update: $e_k = y_k - H_k\hat{x}_k^-$ (29)

Adaptive estimation of measurement noise matrix: (30)

$\hat{M}_k = \frac{1}{N}\sum_{i=k-N+1}^{k} e_i e_i^T$, $\hat{R}_k = \hat{M}_k - H_k P_k^- H_k^T$

Kalman gain matrix update: (31)

$K_k = F_k P_k^-(I - \theta\bar{S}_k P_k^- + H_k^T R_k^{-1} H_k P_k^-)^{-1} H_k^T R_k^{-1}$

Adaptive estimation of process noise matrix: $\hat{Q}_k = K_k\hat{M}_k K_k^T$ (32)

Measurement update of state estimate: $\hat{x}_k^+ = \hat{x}_k^- + K_k e_k$ (33)

Measurement update of error covariance: (34)

$P_k^+ = P_k^-(I - \theta\bar{S}_k P_k^- + H_k^T R_k^{-1} H_k P_k^-)^{-1}$

B. Adaptive H Infinity Filter

Different methods are used to implement the adaptive filter. Mehra [36] divided these methods into four kinds: covariance matching (estimation), correlation, maximum likelihood, and Bayesian. The covariance matching (estimation) is widely adopted in many engineering fields. For example, the AEKF is used to estimate the battery state to improve the estimation accuracy [7]. The AEKF is also applied to control an interior permanent magnet synchronous motor drive for EV traction applications which enhances fault tolerance of position sensor [37]. The adaptive unscented Kalman filter observer is developed to address the NO_x sensor ammonia cross-sensitivity problem with the excellent adaptability for time variation and nonlinear system in [38]. Therefore, an adaptive H infinity filter using the covariance matching technique is adopted to estimate the covariance values to improve its robustness in this study. The realization process is detailed in the following.

1) Updating the Observation Noise Covariance R Adaptively: According to (10), the error innovation can be written as an expression of previous state estimates:

$$e_k = y_k - H_k\hat{x}_k^- = H_k\left(x_k - \hat{x}_k^-\right) + v_k. \quad (14)$$

The variance is taken on both sides of (14) to give the measurement noise covariance

$$M_k = H_k P_k^- H_k^T + R_k \quad (15)$$

where M_k denotes the covariance of e_k and is computed by taking average inside a shifting estimation window of sample N as follows:

$$\hat{M}_k = \frac{1}{N}\sum_{i=k-N+1}^{k} e_i e_i^T. \quad (16)$$

Then, an estimate of R_k is obtained through $\hat{M}_k$ which is the statistical sample variance estimate of M_k

$$\hat{R}_k = \hat{M}_k - H_k P_k^- H_k^T. \quad (17)$$

2) Updating the System Noise Covariance Q Adaptively: Similarly, the process noise w_k is computed from (4)

$$w_k = x_{k+1} - F_k x_k = x_{k+1} - F_k\hat{x}_k^+ + F_k\left(\hat{x}_k^+ - x_k\right). \quad (18)$$

Substituting the state priori estimate (6) into (18) leads to the process noise

$$\begin{aligned} w_k &= x_{k+1} - \hat{x}_{k+1}^- + F_k\left(\hat{x}_k^+ - x_k\right) \\ &= \left(x_{k+1} - \hat{x}_{k+1}^+\right) + F_k\left(\hat{x}_k^+ - x_k\right) + \left(\hat{x}_{k+1}^+ - \hat{x}_{k+1}^-\right). \end{aligned} \quad (19)$$

Then, the variance is taken on both sides of (19) to obtain the system noise matrix

$$\begin{aligned} Q_k = {} & P_{k+1}^+ - F_k P_k^+ F_k^T \\ & + \frac{1}{N}\sum_{i=k-N+1}^{k}\left(\hat{x}_i^+ - \hat{x}_i^-\right)\left(\hat{x}_i^+ - \hat{x}_i^-\right)^T. \end{aligned} \quad (20)$$

In the steady state, only the last term of (20) is considered as an estimate of Q_k, namely

$$\hat{Q}_k = \frac{1}{N}\sum_{i=k-N+1}^{k}\left(\hat{x}_i^+ - \hat{x}_i^-\right)\left(\hat{x}_i^+ - \hat{x}_i^-\right)^T. \quad (21)$$

Substituting (12) and (16) into (21) gives

$$\hat{Q}_k = K_k\hat{M}_k K_k^T. \quad (22)$$

The discrete-time adaptive H infinity filter is shown in Table II, which realizes the real-time adaptive covariance update of both the system and measurement noise.

III. BATTERY MODELING FOR MULTISTATE ESTIMATION

In this section, the battery modeling process will be discussed and the adaptive H infinity filter based battery SOC and SOE estimators will be described.

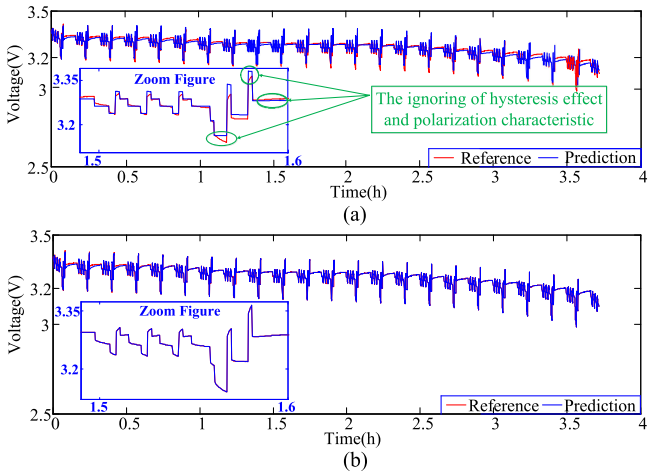

Fig. 1. Terminal voltage estimation results of combined model using: (a) GA. (b) RLS method.

A. Battery Modeling and Parameter Estimation

The combined model is applied to describe the charge/discharge responses of battery terminal voltage, which is shown as follows [4]:

$$U_{t,k} = K_0 - \frac{K_1}{z_k} - K_2 z_k + K_3 \ln(z_k) + K_4 \ln(1 - z_k) - R i_{L,k} \tag{35}$$

where $U_{t,k}$ and $i_{L,k}$ represent the battery terminal voltage and the charge/discharge current at kth sampling moment, respectively. R represents the battery resistance, z represents the battery SOC, and $K_{0,1\ldots4}$ is the fitting coefficients. Usually, $K_{0,1,\ldots,4}$ and R are constant values that are identified offline through the battery dataset. Fig. 1(a) shows the terminal voltage fitting result of the combined model based on one set of LiFePO4 database when the model parameters are identified offline by the genetic algorithm (GA), which is shown as

$$\begin{cases} \min\{f(\hat{\chi}_g)\} \\ \chi = [K_0, K_1, \ldots, K_4, R] \\ f(\hat{\chi}_g) = \sqrt{\frac{1}{N}\sum_{i=1}^{N}\left(U_{t,i} - \hat{U}_{t,i}(\hat{\chi}_g)\right)^2} \end{cases} \tag{36}$$

where the estimate of $U_{t,i}$ at the data point i is denoted as $\hat{U}_{t,i}$, the estimate of the current population χ at generation g is denoted as $\hat{\chi}_g$, and the experimental data length is represented by N. It shows that since the combined model does not consider the hysteresis effect and polarization characteristic of batteries, the model fails to accurately follow the terminal voltage response.

For the purpose of improving the model prediction accuracy without increasing model complexity, the RLS method with a forgetting factor is used to adaptively adjust model parameters according to the observed terminal voltage in real time, where the forgetting factor is able to reduce the influence of outdated data and ensures the high stability of the RLS method. The combined model shown in (35) is the linear discrete input–output equation, the RLS method with a forgetting factor can be directly applied to identify its parameters. Suppose we write (35) into a standard form as

$$y = \phi\theta + w. \tag{37}$$

where y represents the output vector and ϕ and θ represent the input data matrix and the parameter vector, respectively. w represents the white noise vector mainly caused by the measurement. The RLS method to identify the parameter vector θ of the combined model can be shown in the following two steps.

Step 1: Initialization

$$\begin{cases} P_{Ls,0} = 10 \wedge 6 * I,\ \mu = 0.98 \\ \theta_0 = [1, K_{0,0}, K_{1,0}, K_{2,0}, K_{3,0}, K_{4,0}, R_0]^T = [1,0,0,0,0,0]^T \\ \phi_0 = [1, -1/z_0, -z_0, ln(z_0), ln(1-z_0), -i_0] \end{cases} \tag{38}$$

where P_{Ls} denotes the covariance matrix of the estimates; μ denotes the forgetting factor, which is among 0.95 and 1; θ is the parameter vector and K values and R are treated as variables whose initial values are set to zero; ϕ is the input data vector.

Step 2: The Adjustment of θ

$$\begin{cases} K_{Ls,k} = P_{Ls,k-1}\phi_k^T\left[\phi_k P_{Ls,k-1}\phi_k^T + \mu\right]^{-1} \\ \hat{\theta}_k = \hat{\theta}_{k-1} + K_{Ls,k}\left[y_k - \phi_k\hat{\theta}_{k-1}\right] \\ P_{Ls,k} = \frac{1}{\mu}\left[I - K_{Ls,k}\phi_k\right]P_{Ls,k-1} \end{cases} \tag{39}$$

where K_{Ls} is the gain matrix to adaptively adjust θ according to the fitting error between the observed and predicted terminal voltages. In this step, K_{Ls} is first updated mainly based on the covariance matrix P_{Ls} and forgetting factor μ, then the parameter vector θ is adjusted according to the gain matrix K_{Ls} and fitting error. If there is a deviation between the observed and predicted voltages, the covariance matrix P_{Ls} will be large accordingly, which will lead to a big gain matrix K_{Ls} to further reduce the prediction error of terminal voltage by adaptively adjusting the parameter vector θ. In this way, a closed-loop prediction algorithm is constructed to realize the optimal prediction of terminal voltage. Fig. 1(b) is the RLS-based terminal voltage fitting result of the combined model. It can be observed from Fig. 1 that the terminal voltage of the combined model obtained from the RLS method is more accurate than that obtained from the GA, which has demonstrated that the RLS method has improved the estimation accuracy of the combined model than the GA.

B. State-Space Equation Modeling for SOC and SOE Estimation

SOC indicates the remaining charges stored. Mathematically, it can be defined as

$$z_k = z_{k-1} - \frac{\eta_{z,k} i_{L,k} \Delta t}{C_a} \tag{40}$$

where z denotes SOC, C_a denotes the battery total capacity, η_z represents the ampere-hour efficiency which refers to the total discharge capacity divided by the total charge capacity, and Δt denotes the sampling time.

SOE indicates the remaining energy stored in the battery which can be defined as

$$s_k = s_{k-1} - \frac{\eta_{s,k}\Delta E_a}{E_a} = s_{k-1} - \frac{\eta_s U_{t,k-1} i_{L,k}\Delta t}{E_a} \tag{41}$$

where s represents SOE, ΔE_a represents the variation of battery energy between two contiguous sampling times, E_a denotes the battery available energy, and η_s represents the battery energy efficiency, which refers to the total discharge energy divided by the total charge energy.

Combining (35) with (40) gives the state-space model to estimate the SOC

$$\begin{cases} z_k = f\left(z_{k-1}, i_{L,k}\right) + w_{k-1} = z_{k-1} - \frac{\eta_{z,k} i_{L,k}\Delta t}{C_a} + w_{k-1} \\ U_{t,k} = h\left(z_k, i_{L,k}\right) + v_k = K_{0,k} - \frac{K_{1,k}}{z_k} - K_{2,k} z_k \\ \quad + K_{3,k}\ln\left(z_k\right) + K_{4,k}\ln\left(1 - z_k\right) - R_k i_{L,k} + v_k. \end{cases} \tag{42}$$

The Taylor series expansion around the prior state estimation is used to linearize (42) and obtain

$$\begin{cases} x_k = f\left(x_{k-1}, i_{L,k}\right) + w_{k-1} = A_{k-1}x_{k-1} + B_k i_{L,k} + w_{k-1} \\ y_k = h\left(x_k, i_{L,k}\right) + v_k = C_k x_k + D_k i_{L,k} + g_k + v_k \end{cases} \tag{43}$$

where

$$\begin{cases} x_k = z_k, A_{k-1} = 1, B_k = -\frac{\eta_{z,k}\Delta t}{C_a} \\ y_k = U_{t,k}, C_k = \frac{\partial h}{\partial z}\big|_{z=z_k^-} = \frac{K_{1,k}}{z_k^{-2}} - K_{2,k} \\ \quad + \frac{K_{3,k}}{z_k^-} - \frac{K_{4,k}}{1-z_k^-}, D_k = -R_k \\ g_k = K_{0,k} - \frac{K_{1,k}}{z_k^-} - K_{2,k} z_k^- + K_{3,k}\ln\left(z_k^-\right) \\ \quad + K_{4,k}\ln\left(1 - z_k^-\right) + C_k z_k^-. \end{cases} \tag{44}$$

Similar to the SOC state-space equation modeling process, the linearization of the state-space equation to estimate the SOE is the same as (43), but with different coefficients being

$$\begin{cases} x_k = s_k, A_{k-1} = 1, B_k = -\frac{\eta_{s,k} U_{t,k-1}\Delta t}{E_a} \\ y_k = U_{t,k}, C_k = \frac{\partial h}{\partial s}\big|_{s=s_k^-} = \frac{K_{1,k}}{s_k^{-2}} - K_{2,k} \\ \quad + \frac{K_{3,k}}{s_k^-} - \frac{K_{4,k}}{1-s_k^-}, D_k = -R_k \\ g_k = K_{0,k} - \frac{K_{1,k}}{s_k^-} - K_{2,k} s_k^- + K_{3,k}\ln\left(s_k^-\right) \\ \quad + K_{4,k}\ln\left(1 - s_k^-\right) + C_k s_k^-. \end{cases} \tag{45}$$

Both w_k and v_k are random noise terms with unknown statistics and covariance denoted by Q_k and R_k, respectively.

C. Real-Time Multistate Estimation Based on Integration of RLS and Adaptive H Infinity Filter Methods

Fig. 2 shows the SOC and SOE estimator of batteries based on the integration of the RLS and adaptive H infinity filter methods. In order to improve the initial robustness of the proposed approach, the GA-based optimization method has been used to identify the model parameters based on the offline charge/discharge data, which are obtained in the HIL test platform within the first five minutes. Then, these identified parameters are set to the initial model parameters and will be updated in real time for the rest of time. In our experiment, if the estimated states cannot converge to the true values within five minutes, the estimation is considered as a failure. Otherwise, the estimation process will continue.

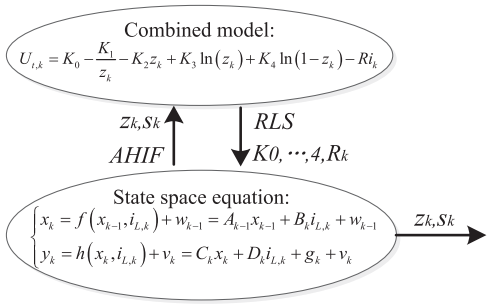

Fig. 2. Multistate estimator based on integration of RLS and adaptive H infinity filter methods.

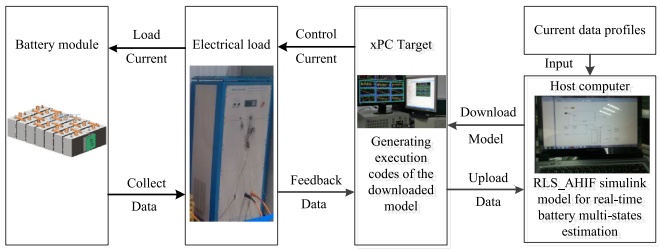

Fig. 3. HIL battery test bench.

First, the RLS method is used to adaptively update the combined model parameters to minimize the terminal voltage error. Then, the adaptive H infinity filter method is executed to estimate battery SOC and SOE based on the battery state-space equation with the identified model parameters. These estimated states including the SOC and the SOE are sent to the RLS calculator as the known inputs for the next time parameter identification. This closed-loop estimation process makes both the adaptive H infinity filter approach to estimate multistates of batteries and the RLS method to identity battery parameters more accurately.

IV. HIL Experimental Approach

The HIL experiments are performed mainly for two purposes: 1) to validate the correctness and effectiveness of the adaptive H infinity filter in real applications; 2) to evaluate the accuracy, robustness, and real-time computing ability of the adaptive H infinity filter based multistate estimator in practice, where the RLS method is applied to identify the battery model parameters in real time. The HIL battery test bench for real-time data collection and computation is shown in Fig. 3, which consists of an electronic load, a host computer, an xPC Target, and the battery pack for charge/discharge. The electronic load specification is listed in Table III. The xPC Target is an industrial personal computer and its specification is shown in Table IV. The battery pack is made up of two same cells in series and the technical specification of each cell is shown in Table V.

First, the controlled current data profiles and the Simulink model for the adaptive H infinity filter based estimators of the SOC and the SOE are downloaded to the xPC target from the host

TABLE III
ELECTRICAL LOAD SPECIFICATION

Item	Range	Accuracy
Current	0–±100 A/0–±200 A	5%(30–200 A)
Voltage(V)	5–16 V/18–500 V	>5%

TABLE IV
IPC SPECIFICATION

Processor system	Max. Speed	Memory (Max. Capacity)
Intel Core 2 Quad	Q9400 2.66 GHz	8 GB

TABLE V
CELL SPECIFICATION

Lithium-ion battery cell	$LiMn_2O_4$
Nominal capacity (Ah)	25
Nominal voltage (V)	3.6
Upper cut-off voltage (V)	4.2
Lower cut-off voltage (V)	2.75

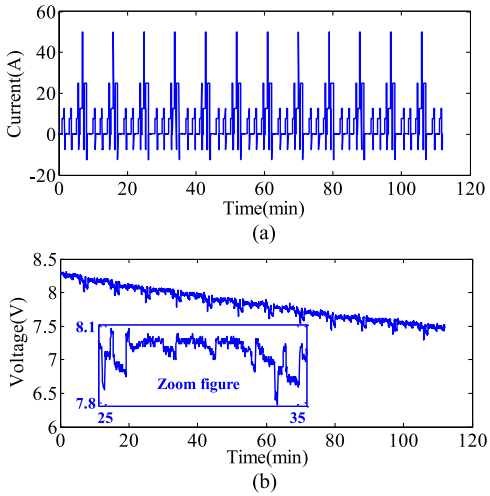

Fig. 4. DST: (a) Current profiles. (b) Voltage profiles.

computer; after compiling the received program, the execution codes are generated and the xPC target will send the current control signals to the electronic load to discharge the battery pack; the real-time collected data including voltage, current, and temperature are then sent back to the xPC target through the electronic load; based on the feedback data, the xPC target will execute the generated codes of the adaptive H infinity filter estimator to estimate the battery SOC and SOE in real time, which will then be used to predict the battery model parameters using the RLS method. The results will be uploaded to the host computer for further processing to better display.

By loading the dynamic stress test (DST) profiles to the battery pack, the collected data of current and voltage are plotted in Fig. 4, where the negative current represents charge and the positive current indicates discharge. From the zoomed figure in Fig. 4(b), it shows that the voltage profiles are strongly influenced by the measurement noise with large fluctuations. It is noted that all the experiments are conducted in the thermal chamber at the constant temperature of 25 °C.

V. EXPERIMENTAL RESULTS

The battery multistate estimation based on the adaptive H infinity filter, EKF, and H infinity filter has been conducted simultaneously in the HIL battery test bench for verification and fair comparison, where the RLS approach is used to make the battery model parameter identification in each method and the capacity and energy efficiencies are assumed to be 100% at the discharge current rate less than 2 C for this Li-ion battery pack in the HIL [6].

There are totally nine design parameters including $P_{Ls,0}$, μ in the RLS algorithm and $\hat{x}_0^+$, $P_0^+, S_0, \tau, Q_0, R_0, N$ in the adaptive H infinity filter. As the initial state vector χ_0 is far away from the real value, $P_{Ls,0}$ will be set as large as 10^6∗I for the quick convergence and μ is usually between 0.95 and 1, which is set to 0.98 in this experiment. $\hat{x}_0^+$ is the initial SOC state, which is set to 80%, 90%, and 100% for the fully charged battery pack, respectively. For the initial SOC of 100%, which is the correct value, P_0^+ should be set as small as zero. For the initial SOCs of 90% and 80%, which are the wrong values, P_0^+ should be respectively increased to 0.01 and 0.04. However, it is found that the SOC estimation will converge to the true value quickly with large P_0^+. Thus, P_0^+ is finally set to 1 in this experiment. Since only one state needs to be estimated by using the adaptive H infinity filter, S_0 will be set to 1. τ indicates model accuracy and smaller τ implies a more accurate state-space model. If the state-space model is believed to be accurate, τ should be set very close to zero. As the accuracy of the combined model has been greatly improved by using the RLS identification in real time, τ is selected to be less than 1. The error of state equation mainly comes from the small sampling error in the measured current and also from the large disturbances in the measured terminal voltage, hence Q_0 is set to be less than 0.01 and R_0 is set to be larger than 1. N is the sampling window length and a reasonable value of N is vital to ensure the filter reliability and accuracy. It is found in the experiment that the filter will obtain better estimation results with N being around 120.

Fig. 5(a) and (b) shows the SOC reference and estimation results and the corresponding estimation errors, respectively. The statistical results of the SOC estimation are listed in Table VI. For the cases where the SOC is intentionally incorrectly set to 90% and 80%, the SOC estimation converges to the true value within 21 and 35 s, respectively. This is because the proposed method can accurately estimate the terminal voltage and adaptively adjust the Kalman gain based on the error between the measured and estimated terminal voltages in real time. In other words, the erroneous SOC setting leads to a large terminal voltage error, which in turn causes a large Kalman gain matrix to compensate the SOC estimation in an efficient closed-loop feedback. After the convergence, the SOC estimation tracks the reference (true) trajectory as accurately as the

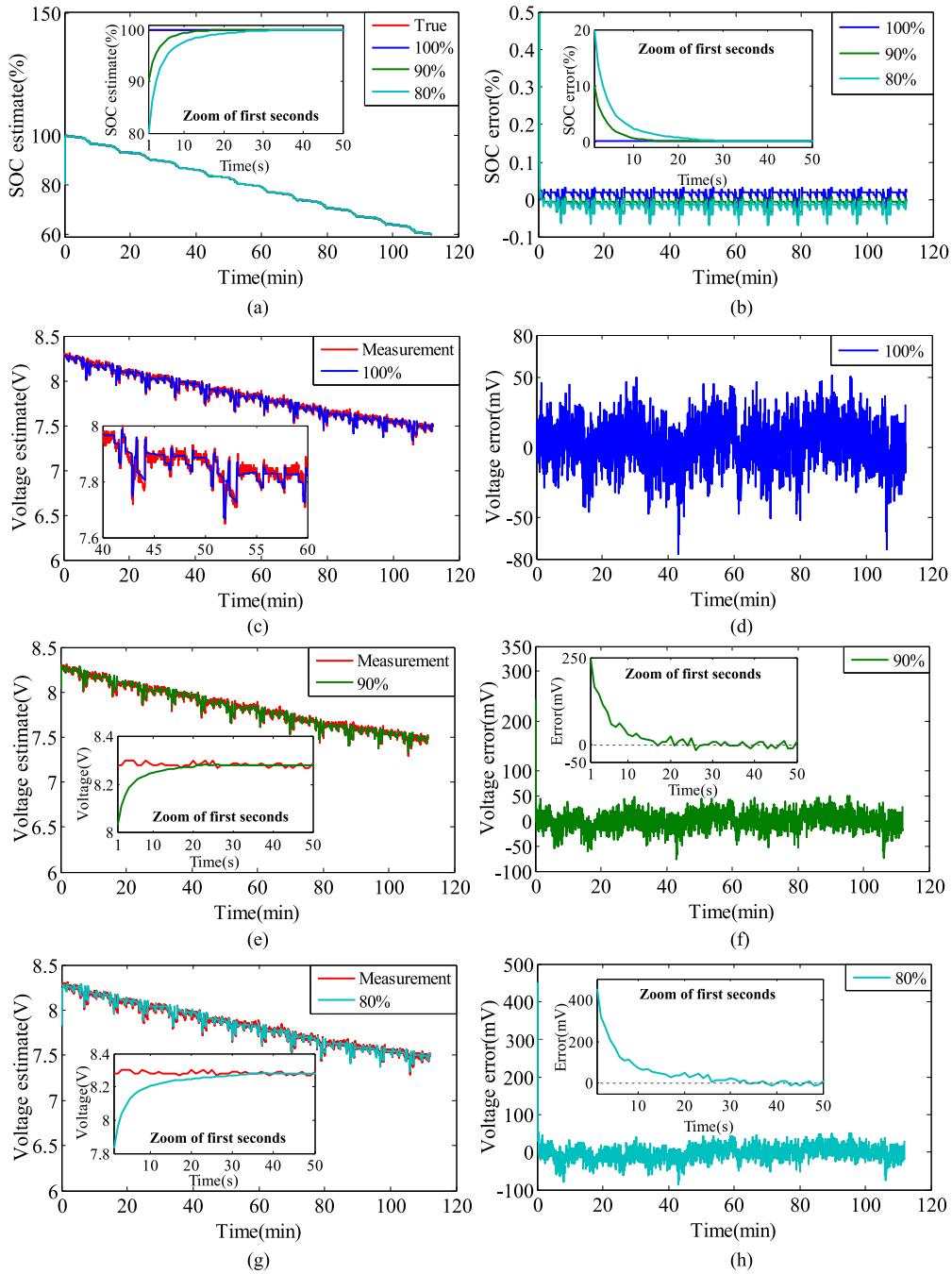

Fig. 5. SOC estimation results with different initial settings of 100%, 90%, and 80% of true initial SOC value based on adaptive H infinite filter: (a) SOC reference and estimation results. (b) SOC estimation error. (c)–(h) Terminal voltage reference and estimation results and terminal voltage estimation errors.

TABLE VI
STATISTICAL RESULTS OF SOC ESTIMATION WITH DIFFERENT INITIAL SETTINGS OF SOC VALUES

Index	Initial SOC	ABSMAX error	Mean error	Standard deviation	Convergence time (s)
SOC(%)	100%	0.04	0.01	0.01	–
	90%	0.06	−0.01	0.01	21
	80%	0.07	−0.02	0.01	35
Voltage(mV)	100%	76.55	2.61	15.08	–
	90%	76.43	0.87	15.92	21
	80%	86.09	−2.65	17.45	35

case of the initial SOC setting of 100%. Take the case of initial SOC of 80% as an example, the absolute maximum (ABSMAX) error, mean error, and standard deviation of the SOC estimation are only 0.07%, –0.02%, and 0.01%, respectively. Fig. 5(c), (e), and (g) shows the measured and estimated terminal voltages and (d), (f), and (h) shows the corresponding estimation voltage errors. It is observed that the terminal voltage estimation errors are up to 250 and 400 mV initially, which are corresponding to the initial incorrect SOC settings of 90% and 80%, respectively. Due to the efficient closed-loop feedback, the estimated terminal voltages converge to the measured terminal voltages

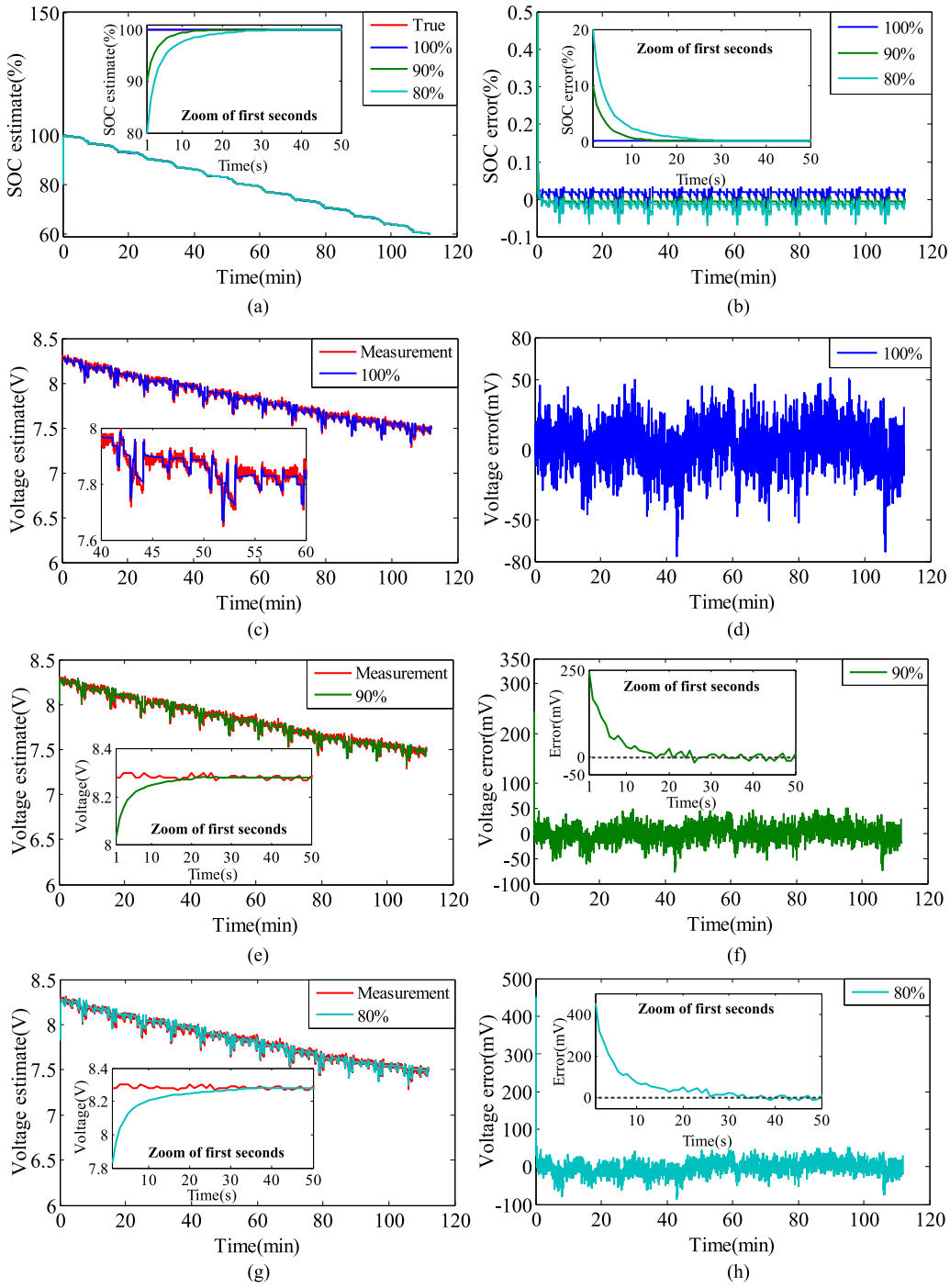

Fig. 6. SOE estimation results with different initial settings of 100%, 90%, and 80% of true initial SOE value based on adaptive H infinite filter: (a) SOE reference and estimation results. (b) SOE estimation error. (c)–(h) Terminal voltage reference and estimation results and terminal voltage estimation errors.

as accurately as the case of the initial SOC setting of 100% after convergence. Furthermore, the estimated voltage tracks the measured voltage accurately with a much smoother trajectory, which indicates the strong noise-filtering ability of the proposed approach. For example, the mean errors of the terminal voltage are only 2.61, 0.87, and –2.65 mV, respectively, for three initial SOC settings of 100%, 90%, and 80%, as shown in Table VI.

The SOE estimation results are shown in Fig. 6, in which the initial SOEs are respectively set to 80%, 90%, and 100% for the fully charged battery pack. Fig. 6(a) and (b) shows the SOE reference and estimation results and the corresponding estimation errors, respectively. For the cases where the SOE is intentionally incorrectly set to 90% and 80%, the SOE estimation converges to the true value within 21 and 62 s, respectively, as shown in Table VII. Take the case of the initial SOE of 80% as an example, the ABSMAX error, mean error, and standard deviation of the SOE estimation are only 0.07%, –0.01%, and 0.01%, respectively, which indicates the high SOE estimation accuracy of

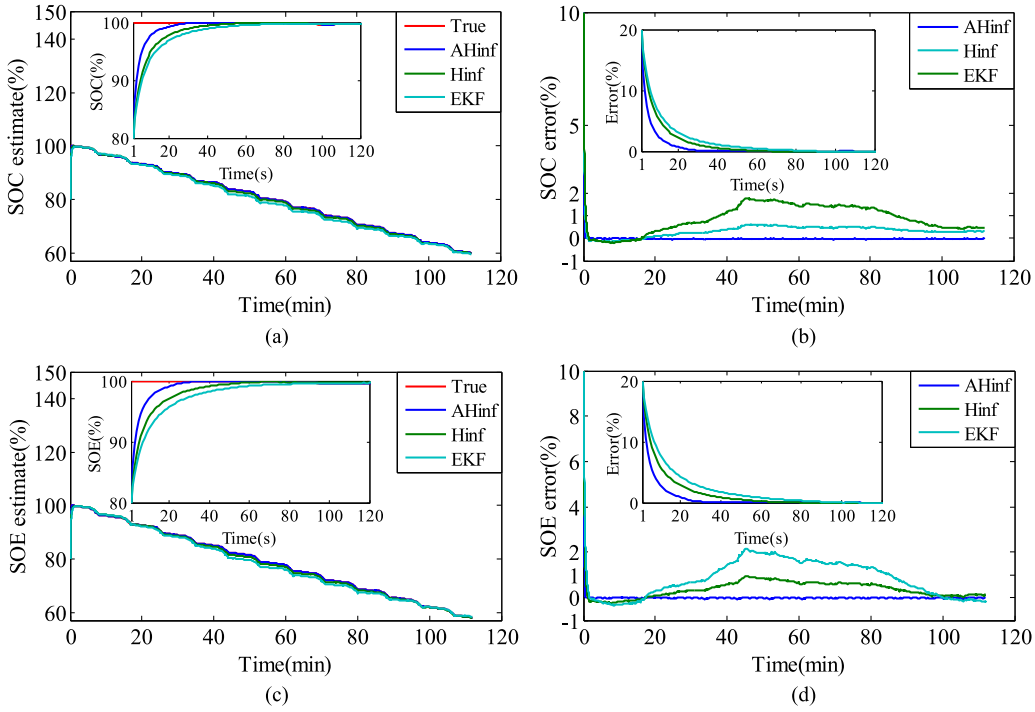

Fig. 7. SOC and SOE estimation results with 80% of their respective true initial SOC and SOE values based on three different filters: (a) SOC reference and estimation results. (b) SOC estimation error. (c) SOE reference and estimation results. (d) SOE estimation error.

TABLE VII
STATISTICAL RESULTS OF SOE ESTIMATION WITH DIFFERENT INITIAL SETTINGS OF SOE VALUES

Index	Initial SOE	ABSMAX error	Mean error	Standard deviation	Convergence time (s)
SOE(%)	100%	0.06	−3e−3	0.01	–
	90%	0.06	−9e−3	0.01	21
	80%	0.07	−0.01	0.01	62
Voltage(mV)	100%	75.54	2.78	15.06	–
	90%	75.48	1.29	15.91	21
	80%	82.99	−2.18	17.49	62

TABLE VIII
STATISTICAL RESULTS OF SOC AND SOE ESTIMATION WITH INITIAL SETTING OF 80% OF THEIR INITIAL VALUES

Index	Filter	ABSMAX error	Mean error	Standard deviation	Convergence time (s)	Average TET (ms)
SOC(%)	AHinf	0.07	−0.02	0.01	35	0.24
	Hinf	0.61	0.31	0.21	67	0.23
	EKF	1.77	0.86	0.59	90	0.23
SOE(%)	AHinf	0.07	−0.01	0.01	62	0.24
	Hinf	0.94	0.36	0.32	77	0.23
	EKF	2.16	0.82	0.77	99	0.23

the proposed method. Fig. 6(c), (e), and (g) shows the measured and estimated terminal voltages and (d), (f), and (h) shows the corresponding estimation errors. Similar to the case of the SOC estimation, after convergence the terminal voltage after filtering is much smoother than the measured voltage, indicating its strong filtering ability against noises. The absolute mean errors are all smaller than 3 mV for the three initial settings of 100%, 90%, and 80%, as shown in Table VII**.**

Thus, the proposed approach is able to estimate the SOC and SOE accurately while obtaining much smother terminal voltage with the high accuracy in real time against inaccurate initial settings of the SOC and SOE values and strong measurement disturbances in the HIL platform.

To further validate the estimation accuracy and stability of the proposed approach, other two traditional filters including the H infinity filter and the EKF are compared in the same HIL platform. Besides the two design parameters $P_{Ls,0}$, μ in the RLS algorithm, there are six design parameters including $\hat{x}_0^+$, $P_0^+, S_0, \tau, Q_0, R_0$ in the H infinity filter and four design parameters including $\hat{x}_0^+$, P_0^+, Q_0, R_0 in the EKF. It is noted that all these parameters follow the same tuning process as described for the adaptive H infinity filter.

The initial SOC and SOE are set to 80% for the three filters, which is 20% away from the true value. Fig. 7(a) and (b) shows the SOC reference and estimation results and corresponding estimation errors, respectively. It is seen that the SOC estimation based on the adaptive H infinity filter, the H infinity filter, and the EKF all converge to the true value gradually with different convergence times of 35, 67, and 90 s, respectively, as shown in Table VIII. It is also seen that the proposed RLS-based model parameter identification method is very effective. For example, the adaptive H infinity filter for the SOC estimation obtains a very small estimation error during the whole filtering time, its ABSMAX error, mean error, and standard deviation are only 0.07%, –0.02%, and 0.01%, respectively, and it is lower than

those of the other two filters. This is because the proposed adaptive H infinity filter is able to adaptively estimate its process noise matrix Q and measurement noise matrix R in real time, making it more robust against noise disturbances in practice. In order to evaluate the operating speed of the proposed method, the average task execution time (TET) of the three filters is also listed in Table VIII, where the average TET is an average of the measured CPU time to run model equations and send out outputs during each sampling interval. It is found that the average TET is 0.24 ms for the adaptive H infinity filter, which is only 0.01 ms longer than the H infinity filter or the EKF and much smaller than 1 s sampling interval in this experiment. Fig. 7(c) and (d) shows the SOE reference and estimation results and corresponding estimation errors. The SOE estimation based on the adaptive H infinity filter converges faster and more accurate than those based on the other two filters. For example, the adaptive H infinity filter has the convergence time of 62 s, which is smaller than 77 and 99 s of the other two filters, its ABSMAX error, mean error, and standard deviation are only 0.07%, –0.01%, and 0.01%, respectively, as shown in Table VIII**.** It indicates that the adaptive infinity filter has higher estimation accuracy than the other two filters. Furthermore, the average TETs for the SOE estimation is the same as those of the SOC estimation for these three filters, indicating that the adaptive H infinity filter for both the SOC and SOE estimation can meet the real-time demand in practice.

VI. Conclusion

In this paper, the adaptive H infinity filter has been employed for battery SOC and SOE estimation with high accuracy and strong robustness to a battery model uncertainty and measurement noise. An HIL experimental platform for battery charge/discharge has been set up to implement the adaptive H infinity filter estimator for battery multistate estimation in real time and validate its effectiveness. The experimental results indicate the excellent performances of the adaptive H infinity filter based estimators with the high estimation accuracy of the SOC and the SOE. The maximum SOC and SOE estimation errors are only 0.04% and 0.06%, respectively, when the initial SOC and SOE are correctly set. When the erroneous initial values of the SOC and the SOE are set to 80% for the fully charged battery pack, the SOC and SOE estimators converge to the true value within 35 and 62 s, respectively, and keep high accuracy within 0.1%. In addition, the proposed estimators have demonstrated strong filtering ability to provide much smoother voltage than the measured voltage.

References

[1] L. Lu, X. Han, J. Li, J. Hua, and M. Ouyang, "A review on the key issues for lithium-ion battery management in electric vehicles," *J. Power Sources*, vol. 226, pp. 272–288, 2013.

[2] K. A. Smith, "Electrochemical control of lithium-ion batteries [applications of control]," *IEEE Control Syst.*, vol. 30, no. 2, pp. 18–25, Apr. 2010.

[3] N. Lotfi, P. Fajri, S. Novosad, J. Savage, R. G. Landers, and M. Ferdowsi, "Development of an experimental testbed for research in lithium-ion battery management systems," *Energies*, vol. 6, pp. 5231–5258, 2013.

[4] G. L. Plett, "Extended Kalman filtering for battery management systems of LiPB-based HEV battery packs: Part 2. Modeling and identification," *J. Power Sources*, vol. 134, no. 2, pp. 262–276, 2004.

[5] X. S. Hu, S. B. Li, and H. Peng, "A comparative study of equivalent circuit models for Li-ion batteries," *J. Power Sources*, vol. 198, pp. 359–367, 2012.

[6] H. He, Y. Zhang, R. Xiong, and C. Wang, "A novel Gaussian model based battery state estimation approach: State-of-Energy," *Appl. Energy*, vol. 151, pp. 41–48, 2015.

[7] J. Han, D. Kim, and M. Sunwoo, "State-of-charge estimation of lead-acid batteries using an adaptive extended Kalman filter," *J. Power Sources*, vol. 188, pp. 606–612, 2009.

[8] Y. J. Wang, C. B. Zhang, and Z. H. Chen, "A method for joint estimation of state-of-charge and available energy of LiFePO4 batteries," *Appl. Energy*, vol. 138, pp. 81–87, 2014.

[9] M. U. Cuma and T. Koroglu, "A comprehensive review on estimation strategies used in hybrid and battery electric vehicles," *Renewable Sustain. Energy Rev.*, vol. 42, pp. 517–531, 2015.

[10] Y. Sun, L. Li, B. J. Yan, C. Yang, and G. Tang, "A hybrid algorithm combining EKF and RLS in synchronous estimation of road grade and vehicle' mass for a hybrid electric bus," *Mech. Syst. Signal Process.*, vol. 68/69, pp. 416–430, 2016.

[11] W. Zhang, W. Shi, and Z. Ma, "Adaptive unscented Kalman filter based state of energy and power capability estimation approach for lithium-ion battery," *J. Power Sources*, vol. 289, pp. 50–62, 2015.

[12] W. Waag, C. Fleischer, and D. U. Sauer, "Critical review of the methods for monitoring of lithium-ion batteries in electric and hybrid vehicles," *J. Power Sources*, vol. 258, pp. 321–339, 2015.

[13] G. L. Plett, "Sigma-point Kalman filtering for battery management systems of LiPB-based HEV battery packs. Part 2: Simultaneous state and parameter estimation," *J. Power Sources*, vol. 161, no. 2, pp. 1369–1384, 2006.

[14] J. H. Meng, G. Z. Luo, and F. Gao, "Lithium polymer battery state-of-charge estimation based on adaptive unscented Kalman filter and support vector machine," *IEEE Trans. Power Electron.*, vol. 31, no. 3, pp. 2226–2238, Mar. 2016.

[15] J. Lee, O. Y. Nam, and B. H. Cho, "Li-ion battery SOC estimation method based on the reduced order extended Kalman filtering," *J. Power Sources*, vol. 174, no. 1, pp. 9–15, 2007.

[16] M. Neumayer, D. Watzenig, and H. Zangl, "An H∞ approach for robust estimation of material parameters in electrical capacitance tomography," *Meas. Sci. Technol.*, vol. 22, no. 10, pp. 1–8, 2011.

[17] W. J. Yang, D. H. Yu, and Y. B. Kim, "Parameter estimation of lithium-ion batteries and noise reduction using an H∞ filter", *J. Mech. Sci. Technol.*, vol. 27, no. 1, pp. 247–256, 2013.

[18] F. Zhang, G. J. Liu, L. J. Fang, and H. Fang, "Estimation of battery state of charge with H∞ observer: Applied to a robot for inspecting power transmission lines," *IEEE Trans. Ind. Electron.*, vol. 59, no. 2, pp. 1086–1095, Feb. 2012.

[19] H. K. Sahoo, P. K. Dashb, and N. P. Rathc, "Frequency estimation of distorted non-stationary signals using complex H∞ filter," *Int. J. Electron. Commun.*, vol. 66, no. 4, pp. 267–274, 2012.

[20] R. Wang, G. P. Liu, W. Wang, D. Rees, and Y.-B. Zhao, "H∞ control for networked predictive control systems based on the switched Lyapunov function method," *IEEE Trans. Ind. Electron.*, vol. 57, no. 10, pp. 3565–3571, Oct. 2010.

[21] X. M. Zhang and Q. L. Han, "Event-based H∞ filtering for sampled-data systems," *Automatica*, vol. 51, pp. 55–69, 2015.

[22] J. Chen, C. B. Ma, and D. Song, "Multiple failure prognosis of landing gear retraction/extension system based on H∞ filtering," *J. Aerosp. Eng.*, vol. 229, no. 8, pp. 1543–1555, 2015.

[23] U. Shaked and N. Berman, "H∞ nonlinear filtering of discrete-time processes," *IEEE Trans. Signal Process.*, vol. 43, no. 9, pp. 2205–2209, Sep. 1995.

[24] G. A. Einicke and L. B. White, "Robust extended Kalman filtering," *IEEE Trans. Signal Process.*, vol. 47, no. 9, pp. 2596–2599, Sep. 1999.

[25] J. Seo, M. J. Yu, C. G. Park, and J. G. Lee, "An extended robust H∞ filter for nonlinear constrained uncertain systems," *IEEE Trans. Signal Process.*, vol. 54, no. 11, pp. 4471–4475, Nov. 2006.

[26] W. L. Li and Y. M. Jia, "H-infinity filtering for a class of nonlinear discrete-time systems based on unscented transform," *Signal Process.*, vol. 90, pp. 3301–3307, 2010.

[27] H. K. Sahoo and P. K. Dash, "Robust estimation of power quality disturbances using unscented H∞ filter," *Int. J. Elect. Power Energy Syst.*, vol. 73, pp. 438–447, 2015.

[28] M. Charkhgard and M. H. Zarif, "Design of adaptive H∞ filter for implementing on state-of-charge estimation based on battery state-of-charge-varying modelling," *IET Power Electron.*, vol. 8, no. 10, pp. 1825–1833, 2015.
[29] N. Lotfi, R. G. Landers, J. Lie, and J. Park, "Electrochemical model-based adaptive estimation of Li-ion battery state of charge," in *ASME Dyn. Syst. Control Conf.*, Columbus, OH, USA, pp. V001T13A008, Oct. 28–30, 2015.
[30] X. J. Dang, L. Yan, K. Xu, X. Wu, H. Jiang, and H. Sun, "Open-circuit voltage-based state of charge estimation of lithium-ion battery using dual neural network fusion battery model," *Electrochim. Acta*, vol. 188, pp. 356–366, 2016.
[31] R. Xiong, F. Sun, X. Gong, and H. He, "Adaptive state of charge estimator for lithium-ion cells series battery pack in electric vehicles," *J. Power Sources*, vol. 242, pp. 699–713, 2013.
[32] F. Sun and R. Xiong, "A novel dual-scale cell state-of-charge estimation approach for series-connected battery pack used in electric vehicles," *J. Power Sources*, vol. 274, pp. 582–594, 2015.
[33] F. Sun, R. Xiong, and H. He, "A systematic state-of-charge estimation framework for multi-cell battery pack in electric vehicles using bias correction technique," *Appl. Energy*, vol. 162, pp 1399–1409, 2016.
[34] G. L. Plett, "Extended Kalman filtering for battery management systems of LiPB-based HEV battery packs: Part 1. Background," *J. Power Sources*, vol. 134, no. 2, pp. 252–261, 2004.
[35] D. Simon, *Optimal State Estimation: Kalman, H∞ and Nonlinear Approaches*. Hoboken, NJ, USA: Wiley, 2006, ch. 11.
[36] R. K. Mehra, "Approaches to adaptive filtering," *IEEE Trans. Automat. Control*, vol. AC-17, no. 5, pp. 693–698, Oct. 1972.
[37] M. Francis and J. Jin-Woo, "Enhanced fault-tolerant control of interior PMSMs based on an adaptive EKF for EV traction applications," *IEEE Trans. Power Electron.*, vol. 31, no. 8, pp. 5746–5758, Aug. 2016.
[38] K. Jiang, E. Cao, and L. J. Wei, "NOx sensor ammonia cross-sensitivity estimation with adaptive unscented Kalman filter for diesel-engine selective catalytic reduction systems," *Fuel*, vol. 165, pp. 185–192, 2016.

Yongzhi Zhang received the B.S. degree in vehicle engineering in 2013 from Chongqing University, Chongqing, China. He is currently working toward the Ph.D. degree in vehicle engineering at Beijing institute of Technology, Beijing, China.

He has published several papers related to estimating battery state. His research mainly focuses on battery state estimation, reliability, and safety.

Rui Xiong (S'12–M'14–SM'16) received the M.Sc. degree in vehicle engineering and the Ph.D. degree in mechanical engineering from Beijing Institute of Technology, Beijing, China, in 2010 and 2014, respectively. He conducted scientific research as a joint Ph.D. student in the DOE GATE Center for Electric Drive Transportation at the University of Michigan, Dearborn, MI, USA, between 2012 and 2014.

Since 2014, he has been an Associate Professor in the Department of Vehicle Engineering, School of Mechanical Engineering, Beijing Institute of Technology, Beijing, China. During 2015, he was a Visiting Associate Professor in the Faculty of Science, Engineering and Technology, Swinburne University of Technology, Hawthorn, Vic., Australia. He has conducted extensive research and authored more than 70 peer-reviewed articles. His research interests mainly include electrical/hybrid vehicles, energy storage, and battery management system.

Dr. Xiong received the Excellent Doctoral Dissertation from Beijing Institute of Technology in 2014 and the first prize of the Chinese Automobile Industry Science and Technology Progress Award in October 2015. He received the Best Paper Awards from the journal Energies in 2015. He is an Associate Editor of the Energy, Ecology and Environment. He serves on the Editorial Board of the Energies.

Hongwen He (M'03–SM'13) received the M.E. degree from Jilin University of Technology, Changchun, China, in 2000 and the Ph.D. degree from Beijing Institute of Technology, Beijing, China, in 2003, both in vehicle engineering.

He is currently a Professor in the National Engineering Laboratory for Electric Vehicles, School of Mechanical Engineering, Beijing Institute of Technology. He has published more than 100 papers and holds nine patents. His research interests include power battery modeling and simulation on electric vehicles, design, and control theory of the hybrid power train.

Dr. He received the first prize of Henan Science and Technology Award for the work on the development of hybrid bus powertrain in 2013, the first prize of Henan Science and Technology Award for the work on the development of battery electric bus powertrain in 2014, and the second prize of Chinese National Science and Technology Award for the work on the development of new energy electric bus powertrains in 2015.

Weixiang Shen (S'00–M'02) received Ph.D. degree in electrical engineering from the University of Hong Kong, Hong Kong, in 2002.

From 2002 to 2003, he was a Lecturer in Ngee Ann Polytechnic, Singapore. From 2003 to 2008, he was a Lecturer and then a Senior Lecturer in the School of Engineering, Monash University, Malaysia. He then worked as a Research Fellow for one year in the School of Electrical and Electronics Engineering, Nanyang Technological University, Singapore. He is currently an Associate Professor of electrical engineering in the Faculty of Science, Engineering and Technology, Swinburne University of Technology, Melbourne, Vic., Australia. His research interests include electric vehicles, renewable energy, and power systems.